Supporting Information

Harvey *et al.* 10.1073/pnas.0804598105

SI Methods

Electrophysiology. Perforated patch-clamp recordings, which prevent the washout of signaling molecules, were performed with a pipette solution containing: 136.5 mM potassium gluconate, 17.5 mM KCl, 9 mM NaCl, 1 mM $MgCl_2$, 10 mM Hepes (pH 7.2), 0.2 mM EGTA and 0.5 mg mL^{-1} amphotericin B (1, 2). Pipettes were front-filled with a small volume of solution lacking amphotericin B. Experiments were performed when the access resistance dropped below 60 MΩ (≈30 min after seal formation). Back-propagating action potentials (Fig. 4) were triggered by current injections (2–4 nA, 2 ms) at the soma. Glutamate receptor blockers (10 μM NBQX and 5 μM CPP) were included in the bath during back-propagating action potential experiments. Synaptic stimulation (Fig. 5) was performed using short current pulses (0.1 ms) delivered with a glass pipette (≈2- to 3-μm tip diameter) filled with ACSF. The pipette was positioned in the apical dendrites ≈150 μm from the soma. The stimulus strength was set to produce an excitatory postsynaptic potential (EPSP) of ≈5–8 mV. The theta-burst protocol consisted of a burst of 5 synaptic stimuli at 100 Hz, repeated 10 times at 5 Hz. The set of 10 bursts was repeated 3 times at 10-second intervals. Picrotoxin (100 μm), to prevent inhibition, and 2-chloroadenosine (2 μm), to reduce recurrent activity, were included in the bath during synaptic stimulation.

Biochemistry. COS7 cells were cultured in DMEM with 10% FBS and were transfected with $EKAR_{cyto}$ using Lipofectamine. The expression vectors for constitutively active MEK (DN-MEK-EE) and MKP1 have been described previously (3, 4). For UV treatment (Fig. 3*C*), cells were irradiated with 60 J/m^2 UV-C and then incubated for 1 h before lysis. For PMA stimulation experiments (Fig. 3*B*), cells were serum-starved for 12 h starting at 36 h after transfection and were lysed following PMA application (1 μM, 10 min). The lysis buffer contained: 25 mM Hepes (pH 7.5), 134 mM NaCl, 10% glycerol, 1% Triton X-100, 25 mM β-glycerophosphate, 2 mM EDTA, 100 μM Na orthovanadate, 10 mM PMSF, 10 μg/ml leupeptin and 10 μM aprotinin. Western blots were analyzed using chemiluminescence detection and were quantified in ImageJ. $EKAR_{cyto}$ phosphorylation was measured at its Cdc25C substrate peptide. Phospho-Cdc25C signals from $EKAR_{cyto}$ and from endogenous Cdc25C were distinguished based on protein size. Relative phosphorylation was calculated as the ratio of phosphorylated protein to total protein from the same sample; each intensity measurement is therefore independent of sample-to-sample variations in protein levels. The antibodies used were: GFP (Roche), ERK1/2 (Santa Cruz Biotechnology), *p*-ERK1/2 (Cell Signaling Technology), *p*-JNK (Cell Signaling Technology), *p*-p38 (Cell Signaling Technology), and *p*-Thr-48-Cdc25C (Cell Signaling Technology). Phorbol myristate acetate (PMA) was purchased from Sigma. U0126, SP600125, and PD169316 were purchased from Calbiochem. U0126, SP600125, and PD169316 (a pyridinyl imidazole compound similar to SB203580) are selective antagonists of MKK1, JNK, and p38, respectively (5, 6).

FLIM Data Analysis. We used fluorescence lifetime measurements to quantify the FRET signals reported by EKAR. Following pulsed excitation with a mode-locked Ti:sapphire laser (80-MHz pulse frequency), a fluorescence decay curve, $F(t)$, was obtained from a histogram of photon arrival times, measured as the time between photon signals and laser pulses using time-correlated single photon counting (TCSPC) (1, 7, 8). The fluorescence lifetime can be obtained from the mean photon arrival time, where the mean photon arrival time, $\langle t \rangle$, is measured as (7):

$$\langle t \rangle = \frac{\int dt \cdot tF(t)}{\int dt \cdot F(t)} \quad [1]$$

The mean photon arrival time is related to the fluorescence lifetime, $\langle \tau \rangle$, by an offset arrival time, t_o, that depends on the position of the sample:

$$\langle \tau \rangle = \langle t \rangle - t_0 \quad [2]$$

First it is necessary to estimate the offset arrival time. We therefore calculated the fluorescence lifetime from a fit of the fluorescence decay curve. We assumed that the fluorescence decay curve, $F(t)$, was composed of 2 populations, free donors (P_D) and donors bound to acceptor (P_{AD}), with fluorescence lifetimes τ_D and τ_{AD}, respectively:

$$F(t) = F_o[P_D \exp(-t/\tau_D) + P_{AD} \exp(-t/\tau_{AD})] \quad [3]$$

However, in TCSPC measurements, the fluorescence decay curve is convolved with the pulse response function (PRF) of the microscope, which is the uncertainty in the arrival times of photons mostly due to the transit time spread of the PMT (assumed to be Gaussian with width τ_G) (1). The fluorescence decay curve therefore can be expressed as:

$$F(t,t_0, \tau_D, \tau_G, \tau_{AD}, P_D, P_{AD}) = F_0[P_D \cdot G(t, t_0, \tau_D, \tau_G) + P_{AD} \cdot G(t, t_0, \tau_{AD}, \tau_G)] \quad [4]$$

where G is the convolution of the Gaussian PRF and an exponential decay:

$$G(t, t_0, \tau_D, \tau_G) = \frac{1}{2} \exp\left(\frac{\tau_G^2}{2\tau_D} - \frac{t - t_0}{\tau_D}\right) \operatorname{erf}\left(\frac{\tau_G^2 - \tau_D(t - t_0)}{\sqrt{2}\tau_D \tau_G}\right) \quad [5]$$

We fit Eq. **4** with 2 exponentials with time constants τ_D and τ_{AD}. The fit was constrained by fixing τ_D and τ_G to values obtained under favorable conditions in HEK293 (τ_D = 2.53 ns for EGFP and 3.02 ns for Venus, and τ_G = 0.157 ns) (1). From the fit, we calculated the mean fluorescence lifetime, where the theoretical average for multiple populations (i.e., free donors and donors bound to acceptors) is given by:

$$\langle \tau \rangle \sim \frac{\int dt \cdot [P_D \cdot \exp(-t/\tau_D) + P_{AD} \cdot \exp(-t/\tau_{AD})]}{\int dt \cdot [P_D \cdot \exp(-t/\tau_D) + P_{AD} \cdot \exp(-t/\tau_{AD})]} \sim \frac{P_D \tau_D^2 + P_{AD} \tau_{AD}^2}{P_D \tau_D + P_{AD} \tau_{AD}} \quad [6]$$

For each experiment, we calculated the fluorescence lifetime for multiple images (range 3–4) by fitting in this manner and

compared these values with the mean photon arrival times to estimate the offset arrival time using Eq. **2**. The average offset arrival time was used for all images in an experiment. All fluorescence lifetime values were then obtained from the mean photon arrival time (Eq. **1**) using the calculated offset (Eq. **2**). This method was also used to estimate the fluorescence lifetime of the CFP-YFP version of EKAR (Table S1), even though Cerulean has a fluorescence decay curve with multiple time constants (1).

In certain experimental cases, determining the fluorescence lifetime and binding fraction (P_{AD}) from fitting is preferable to using the mean photon arrival time (1). With sensors like EKAR, however, 3 populations of donors with different lifetimes are present: donors not bound to acceptors, donors bound to acceptors, and donors in a molecule without a functional acceptor chromophore. The third population is likely a significant fraction of the sensor molecules because only ≈50% of mRFP1 molecules function as acceptors (1). Since fitting can be unstable with 3 populations, the mean photon arrival time method therefore is preferable here.

SNR Comparison of FLIM and Intensity-Based Measurements. HEK293 cells were transfected with the CFP-YFP version of $EKAR_{cyto}$ and stimulated with EGF, as described above. For each sample, FLIM images and intensity images were interleaved and acquired following 2-photon excitation with 800-nm light. The excitation and detection parameters were identical for both sets of images. For intensity-based measurements, the SNR was defined as the maximum YFP/CFP ratio change, normalized to the baseline ratio ($\Delta R/R$), divided by the standard deviation of $\Delta R/R$ for baseline images. No corrections were made for spectral bleed-through. For FLIM measurements, the SNR was defined as the maximum fluorescence lifetime change divided by the standard deviation of the baseline fluorescence lifetime changes. Eight baseline time points were acquired for each experiment. The maximum ratio and lifetime changes were obtained within 20 min after the addition of EGF.

Ratio images (Fig. 7*A*) were created by dividing the YFP signal by the CFP signal pixel-by-pixel following low-pass filtering of the YFP and CFP images. Only pixels with a value greater than the mean background signal plus 4 times the standard deviation of the background signal were included in the ratio images. CFP FLIM images were created using only the mean photon arrival time, without correction for the sample position using an offset arrival time, t_o. Because Cerulean has a fluorescence decay curve with multiple time constants even in the absence of acceptor (1), stable curve-fitting to estimate the fluorescence lifetime and the offset arrival time were not possible. Since the offset arrival time is constant for a given sample, the absolute changes in the mean photon arrival time are the same as the absolute changes in fluorescence lifetime (see Eq. **2**). Therefore, CFP FLIM images (Fig. 7*A*) illustrate the fluorescence lifetime changes, but the values provided (in nanoseconds) are mean photon arrival times and do not accurately reflect fluorescence lifetime values.

SI Discussion

Optimization of EKAR's Signal. The mature form of EKAR resulted from a screen of numerous sensors, using the EGF stimulation of HEK293 cells as a fast and robust assay to optimize the components of EKAR (i.e., FRET pairs, phospho-binding domains, substrate peptides, and linkers). See Table S1 for a summary of the sensors tested.

The EGFP-mRFP1 FRET pair was selected because it is a combination well-suited for 2pFLIM (9) that provided a large fluorescence lifetime change. Other fluorescent protein combinations, such as circularly permuted forms of Venus (10–12) paired with mRFP1, provided minor improvements in the signal (Table S1). However, because EGFP was brighter than Venus under 2-photon excitation in our setup (1), we chose the EGFP-mRFP1 pair. Other FRET pairs, such as Venus-mRFP1, Venus-hcRed, and EGFP-mCherry, did not provide larger signals. For ratiometric FRET measurements, other FRET pairs, such as CFP-YFP combinations, may be preferable (Fig. 2*C*). Also, the incorporation of new FRET pairs (13, 14) may improve EKAR's signal.

Several phospho-binding domains and substrate peptides were tested. The WW domain-Cdc25C peptide combination provided the largest signal while maintaining rapid reversibility. The binding affinity between these 2 domains ($K_D \approx 8\ \mu M$) (15) is a major determinant of reversibility, such that low affinities allow phosphatases to act on the sensor (16). Low affinities therefore produce sensors with kinetics that resemble the activity patterns of the endogenous kinase. High affinities can also be useful to produce irreversible sensors with larger signals for cases in which the activity kinetics are not important. This situation is similar to the use of indicators with differing affinities in $[Ca^{2+}]$ imaging (17). Because the crystal structure of the WW-phosphopeptide interface has been solved (15), the design of EKAR variants with a broad range of affinities should be possible. Other less successful combinations were also tested: the Cdc25C peptide paired with the FHA phospho-binding domain and the ERK substrate RSK2 (amino acids 560–740) combined with the WW domain.

Optimization of the linker regions greatly enhanced the sensor's signal. In addition to optimizing the central linker (Fig. 2*E*), we also varied the length of the linkers adjacent to the fluorescent proteins. We found that shorter linkers, consisting of only several amino acids, provided the largest signals. Finally, we attempted to decrease the baseline FRET by modifying the central linker to increase the distance between the fluorescent proteins (18). However, the placement of rigid α-helices or α-helices in combination with flexible linkers was unsuccessful in this aim.

Different sensor designs were also tested. First, ERK undergoes a conformational change upon activation due to the unbinding of MEK (19). Such a conformational change may alter FRET. However, placement of mRFP1 and EGFP at the N and C terminus of ERK, respectively, resulted in only a small FRET change upon EGF stimulation. Second, ERK may dimerize upon activation (20). We made an intramolecular sensor containing mRFP1-ERK and EGFP-ERK joined by a flexible linker; however, this sensor showed no stimulus-dependent FRET change.

Comparison of Ratio and Lifetime Changes with FRET. EKAR undergoes a ≈2–3% decrease in fluorescence lifetime and a ≈20% increase in acceptor-to-donor fluorescence ratio following various stimuli (e.g., Fig. 2). Is this relationship between lifetime and ratio changes expected for a FRET change? We estimated the relationship between percent ratio and lifetime changes following increases in binding fraction (P_{AD}). In ratiometric measurements, the fluorescence in the donor (F_D) and acceptor (F_{AD}) channels can be calculated as (21):

$$F_D = F_D^{\text{no FRET}}(1 - Y_{\text{FRET}} \cdot P_{AD}) \quad [7]$$

$$F_A = F_D^{\text{no FRET}} \cdot \alpha \cdot Y_{\text{FRET}} \cdot P_{AD} + F_D \cdot R_{BT} + F_A^{\text{Direct}} \quad [8]$$

where F_D^{noFRET} is the donor fluorescence without FRET, α is the ratio of the acceptor-to-donor quantum yields, R_{BT} is the fraction of bleed-through from the donor channel into the acceptor channel, F_A^{Direct} is the acceptor fluorescence due to direct excitation, and Y_{FRET} is the FRET efficiency. We can calculate the mean fluorescence lifetime, $\langle\tau\rangle$, using Eq. **6**, in which τ_D and τ_{AD} are the lifetimes of free donors and donors bound to acceptors, respectively. Here we assume that there are only 2 populations of donors.

Since Cerulean, the donor in the CFP-YFP version of EKAR, has a fluorescence decay curve with multiple time constants (1), it is difficult to estimate τ_D and τ_{AD} from fitting and therefore to estimate percent lifetime changes. We instead used values for a EGFP-mRFP1 pair. We used $\alpha = 0.4$ (22), $R_{BT} = 0.1$ (23), and $F_A^{\text{Direct}}/F_D^{\text{noFRET}} = 0.03$ (23), following previous measurements and simulations (21). For EGFP $\tau_D = 2.59$ ns (1), and from fitting (Eq. **4**) we estimated $\tau_{AD} = 1.1$. Since

$$Y_{\text{FRET}} = 1 - \frac{\tau_{AD}}{\tau_D} \quad [9]$$

we estimated $Y_{\text{FRET}} = 0.57$.

We set the initial binding fraction to 0.25 since

$$P_{AD} = \frac{\tau_D(\tau_D - \langle\tau\rangle)}{\tau_D(\tau_D - \langle\tau\rangle) + \tau_{AD}(\langle\tau\rangle - \tau_{AD})} \quad [10]$$

and $\langle\tau\rangle$ in the resting state for EKAR is ≈2.4 ns (Table S1). We calculated the percent lifetime and ratio changes following binding fraction increases between Δbinding fraction = 0 and Δbinding fraction = 0.2. For a fluorescence lifetime decrease of ≈3%, an acceptor-to-donor fluorescence ratio increase of ≈15% is expected (Fig. S2). For a CFP-YFP pair with $\alpha = 1.5$ (24), $R_{BT} = 0.2$ (24), and $F_A^{\text{Direct}}/F_D^{\text{noFRET}} = 0.03$ (23), a ratio increase of ≈20% is expected, assuming the same FRET efficiency. We therefore conclude that our experimentally measured relationship between lifetime and ratio changes is within an expected range for FRET changes.

1. Yasuda R, *et al.* (2006) Supersensitive Ras activation in dendrites and spines revealed by two-photon fluorescence lifetime imaging. *Nat Neurosci* 9:283–291.
2. Harvey CD, Svoboda K (2007) Locally dynamic synaptic learning rules in pyramidal neuron dendrites. *Nature* 450:1195–1200.
3. Mansour SJ, *et al.* (1994) Transformation of mammalian cells by constitutively active MAP kinase kinase. *Science* 265:966–970.
4. Gupta S, *et al.* (1996) Selective interaction of JNK protein kinase isoforms with transcription factors. *EMBO J* 15:2760–2770.
5. Bennett BL, *et al.* (2001) SP600125, an anthrapyrazolone inhibitor of Jun N-terminal kinase. *Proc Natl Acad Sci USA* 98:13681–13686.
6. Davies SP, Reddy H, Caivano M, Cohen P (2000) Specificity and mechanism of action of some commonly used protein kinase inhibitors. *Biochem J* 351:95–105.
7. Lakowicz JR (1999) *Principles of Fluorescence Spectroscopy* (Plenum, New York).
8. Becker W, *et al.* (2004) Fluorescence lifetime imaging by time-correlated single-photon counting. *Microsc Res Tech* 63:58–66.
9. Peter M, *et al.* (2005) Multiphoton-FLIM quantification of the EGFP-mRFP1 FRET pair for localization of membrane receptor-kinase interactions. *Biophys J* 88:1224–1237.
10. Baird GS, Zacharias DA, Tsien RY (1999) Circular permutation and receptor insertion within green fluorescent proteins. *Proc Natl Acad Sci USA* 96:11241–11246.
11. Nagai T, Sawano A, Park ES, Miyawaki A (2001) Circularly permuted green fluorescent proteins engineered to sense Ca2+. *Proc Natl Acad Sci USA* 98:3197–3202.
12. Nagai T, *et al.* (2004) Expanded dynamic range of fluorescent indicators for Ca2+ by circularly permuted yellow fluorescent proteins. *Proc Natl Acad Sci USA* 101:10554–10559.
13. Nguyen AW, Daugherty PS (2005) Evolutionary optimization of fluorescent proteins for intracellular FRET. *Nat Biotechnol* 23:355–360.
14. Ganesan S, *et al.* (2006) A dark yellow fluorescent protein (YFP)-based resonance energy-accepting chromoprotein (REACh) for Forster resonance energy transfer with GFP. *Proc Natl Acad Sci USA* 103:4089–14094.
15. Verdecia MA, *et al.* (2000) Structural basis for phosphoserine-proline recognition by group IV WW domains. *Nat Struct Biol* 7:639–643.
16. Zhang J, *et al.* (2005) Insulin disrupts beta-adrenergic signalling to protein kinase A in adipocytes. *Nature* 437:569–573.
17. Yasuda R, *et al.* (2004) Imaging calcium concentration dynamics in small neuronal compartments. *Sci STKE* 2004:pl5.
18. Arai R, *et al.* (2001) Design of the linkers which effectively separate domains of a bifunctional fusion protein. *Protein Eng* 14:529–532.
19. Fujioka A, *et al.* (2006) Dynamics of the Ras/ERK MAPK cascade as monitored by fluorescent probes. *J Biol Chem* 281:8917–8926.
20. Khokhlatchev AV, *et al.* (1998) Phosphorylation of the MAP kinase ERK2 promotes its homodimerization and nuclear translocation. *Cell* 93:605–615.
21. Yasuda R (2006) Imaging spatiotemporal dynamics of neuronal signaling using fluorescence resonance energy transfer and fluorescence lifetime imaging microscopy. *Curr Opin Neurobiol* 16:551–561.
22. Campbell RE, *et al.* (2002) A monomeric red fluorescent protein. *Proc Natl Acad Sci USA* 99:7877–7882.
23. Erickson MG, Moon DL, Yue DT (2003) DsRed as a potential FRET partner with CFP and GFP. *Biophys J* 85:599–611.
24. Tsien RY (1998) The green fluorescent protein. *Annu Rev Biochem* 67:509–544.
25. Sato M, *et al.* (2002) Fluorescent indicators for imaging protein phosphorylation in single living cells. *Nat Biotechnol* 20:287–294.
26. Mori MX, Erickson MG, Yue DT (2004) Functional stoichiometry and local enrichment of calmodulin interacting with Ca2+ channels. *Science* 304:432–435.

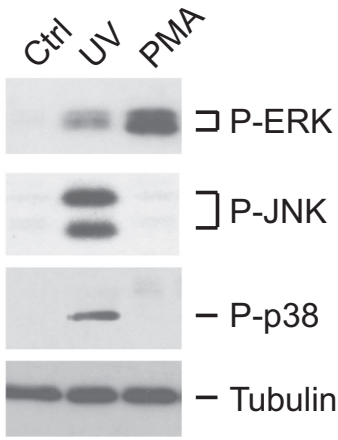

Fig. S1. Effect of UV and phorbol ester stimulation on MAPK activity in COS7 cells. COS7 cells were treated with 60 J/m^2 UV-C and then incubated for 1 h or treated with the phorbol ester PMA (1 μM) for 10 min. Protein extracts were examined by immunoblot analysis with antibodies to phospho-ERK, phospho-JNK, phospho-p38, and tubulin.

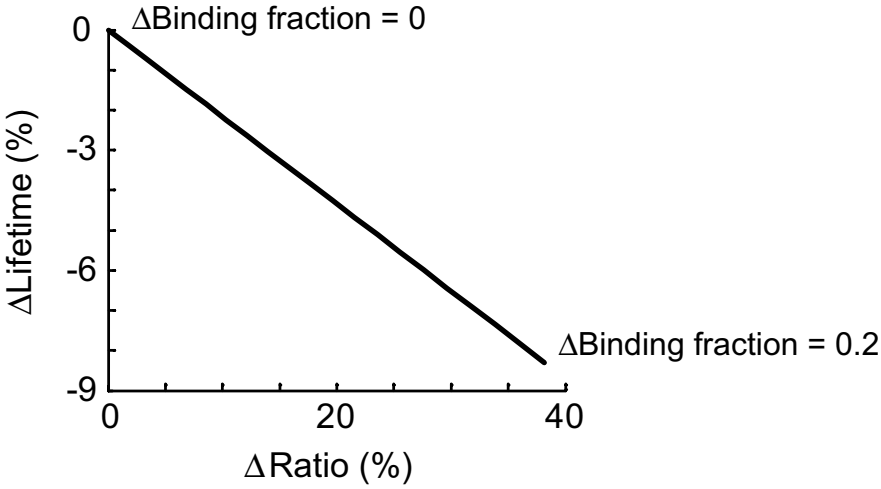

Fig. S2. Estimated percent changes in fluorescence lifetime and acceptor-to-donor fluorescence ratio for increases in binding fraction. Values are estimated for a EGFP-mRFP1 FRET pair. See *SI Text* for details.

Table S1. summary of tested sensors

	Baseline lifetime, ns	ΔLifetime[c], ns	ΔLifetime [c], %	Notes[d]
EKAR variants[a]				
EKAR cytoplasmic	2.41 ± 0.01	−0.071 ± 0.002	−2.92 ± 0.07	
EKAR nuclear	2.39 ± 0.01	−0.069 ± 0.003	−2.89 ± 0.15	
Intermolecular EKAR	2.56 ± 0.01	−0.009 ± 0.003	−0.35 ± 0.11	Cytoplasmic mRFP1-WW + Cdc25C-EGFP
FRET pairs[b]				
mRFP1-mRFP1-EGFP	2.28 ± 0.02	−0.073 ± 0.002	−3.20 ± 0.07	Two N-terminal copies of mRFP1
mRFP1-mVenus	2.79 ± 0.01	−0.051 ± 0.003	−1.82 ± 0.12	
mRFP1-cp49 Venus	2.93 ± 0.01	−0.094 ± 0.004	−3.21 ± 0.13	Nagai *et al.* (2004) *Proc Natl Acad Sci USA*
mRFP1-cp157 Venus	2.85 ± 0.02	−0.090 ± 0.008	−3.14 ± 0.31	Nagai *et al.* (2004) *Proc Natl Acad Sci USA*
mRFP1-cp173 Venus	2.77 ± 0.02	−0.070 ± 0.011	−2.53 ± 0.37	Nagai *et al.* (2004) *Proc Natl Acad Sci USA*
mRFP1-cp195 Venus	2.86 ± 0.01	−0.059 ± 0.007	−2.06 ± 0.27	Nagai *et al.* (2004) *Proc Natl Acad Sci USA*
mRFP1-cp229 Venus	2.88 ± 0.02	−0.070 ± 0.006	−2.44 ± 0.20	Nagai *et al.* (2004) *Proc Natl Acad Sci USA*
hcRed-Venus	2.83 ± 0.03	−0.017 ± 0.007	−0.58 ± 0.24	
mCherry-EGFP	2.43 ± 0.01	−0.068 ± 0.004	−2.80 ± 0.10	
EGFP-mRFP1	2.42 ± 0.01	−0.067 ± 0.001	−2.77 ± 0.06	Swap FP position in EKAR
mCerulean-mVenus	2.61 ± 0.03	−0.073 ± 0.009	−2.80 ± 0.34	
Phospho-binding and substrate peptides				
FHA phospho binding	2.47 ± 0.01	−0.032 ± 0.003	−1.31 ± 0.12	
RSK2 substrate	2.57 ± 0.01	−0.004 ± 0.002	−0.16 ± 0.10	Mouse RSK2 aa 560–740
Linkers				
Long linkers adjacent to FPs	2.43 ± 0.02	−0.015 ± 0.004	−0.63 ± 0.15	≈15-aa random sequence
9-aa central linker	2.36 ± 0.01	−0.041 ± 0.005	−1.72 ± 0.18	Sato *et al.* (2002) *Nat Biotechnol*
192 Gly linker	2.35 ± 0.01	−0.039 ± 0.004	−1.66 ± 0.17	Mori *et al.* (2004) *Science*
384 Gly linker	2.30 ± 0.02	−0.026 ± 0.007	−1.13 ± 0.20	Mori *et al.* (2004) *Science*
Helix central linker	2.35 ± 0.01	−0.052 ± 0.004	−2.21 ± 0.14	Arai *et al.* (2001) *Protein Eng*
Helix–Gly–Helix central linker	2.30 ± 0.03	−0.035 ± 0.006	−1.54 ± 0.19	
Gly–Helix–Gly central linker	2.33 ± 0.01	−0.038 ± 0.005	−1.63 ± 0.23	
Docking domains				
Cdc25C-FAFP	2.40 ± 0.02	−0.062 ± 0.004	−2.59 ± 0.17	
Cdc25C-FQAP	2.41 ± 0.02	−0.024 ± 0.005	−0.99 ± 0.22	
Cdc25C-ATAP	2.38 ± 0.02	−0.010 ± 0.003	−0.42 ± 0.11	
FQFP-Cdc25C-FQFP	2.36 ± 0.01	−0.068 ± 0.007	−2.89 ± 0.13	
Cdc25C-FQFP-FQFP	2.33 ± 0.01	−0.051 ± 0.010	−2.16 ± 0.31	
Cdc25C-linker-FQFP	2.44 ± 0.01	−0.026 ± 0.008	−1.08 ± 0.25	
Other sensor designs				
ERK dimerization	2.39 ± 0.01	−0.005 ± 0.002	−0.21 ± 0.09	mRFP-ERK-linker-EGFP-ERK
mRFP1-ERK-EGFP	2.41 ± 0.01	+0.013 ± 0.005	+0.56 ± 0.17	Based on Miu2; Fujioka *et al.* (2006) *J Biol Chem*

All data are mean ± SEM.

[a]All variants are version of nuclear EKAR with 1 component changed.

[b]The N-terminal fluorescent protein (FP) is listed first and the C-terminal FP is listed second (e.g. for EKAR: mRFP1-EGFP).

[c]Lifetime changes were measured in HEK293 cells following application of 100 ng/ml EGF.

[d]See references in *SI Text* for full citations.